PHYSICAL REVIEW A VOLUME 49, NUMBER 1 JANUARY 1994

Systematics and scaling of differential ionization cross sections in multicharged ion-atom collisions

R. D. DuBois, L. H. Toburen, and M. E. Middendorf
Pacific Northwest Laboratory, Richland, Washington 99352

O. Jagutzki
Institute für Kernphysik der Johann-Wolfgang-Goethe-Universität Frankfurt, D-6000 Frankfurt am Main, Germany
(Received 8 February 1993)

Absolute doubly differential cross sections for electron emission are presented for 0.5-MeV/u multicharged ion-atom collisions. The collision systems investigated are B^{q+}, C^{q+} ($q=2-5$) and O^{q+}, F^{q+} ($q=3-6$) projectiles impacting on helium and C^{q+} ($q=2-5$) ions impacting on neon and argon targets. Laboratory electron emission angles between 10° and 60° were studied. Under the assumption that the cross sections scale with the square of an effective projectile charge, $Z_{\text{eff}}(\varepsilon,\theta)$, the scaling was investigated as a function of emitted electron velocity and angle. For distant collisions (low-energy electron emission), we find that $Z_{\text{eff}}(\varepsilon,\theta)>q$ for small q. For the highest values of q investigated, $Z_{\text{eff}}(\varepsilon,\theta)$ was found to be smaller than the net projectile charge q. The effective projectile charges may be subject to a systematic underestimation since they were determined by referencing the partially stripped ion impact data to fully stripped boron, rather than proton, impact cross sections. In the binary-encounter region, the present data confirm previously observed features—namely that the emission increases as q decreases. For the helium target, the qualitative behavior is roughly in accordance with predictions by Schulz and Olson [J. Phys. B **24**, 3409 (1991)]. Neon and argon targets also demonstrate these features, but less dramatically than helium.

PACS number(s): 34.50.Fa

INTRODUCTION

Differential electron emission studies provide a very sensitive probe for investigating interactions between atomic particles. For single ionization of simple atoms by protons, it has been shown [1] that the first Born approximation is reasonably accurate in describing interactions where the impact energy is larger than a few hundred keV. For higher Z, fully stripped projectile impact, the differential electron emission cross sections for single ionization are expected to scale as Z^2. For *very* high Z projectiles, deviations from Z^2 scaling are known to occur [2–6].

The situation is much more complicated if the projectiles contain bound electrons of their own. These bound electrons can also participate in the collision, either actively, which increases the cross section for electron production, or passively, which typically reduces the cross section with respect to that resulting from fully stripped ion impact. One active role is ionization of the projectile electrons, which from a theoretical viewpoint is equivalent to target ionization induced by neutral projectile impact. Thus, understanding the active role leading to projectile ionization is equivalent to understanding the passive role bound electrons play in ionization of a target by dressed-ion impact.

An additional, and more complicated, active role involves direct interactions between projectile and target electrons. These interactions lead to both electrons being ionized and/or excited. Two-center electron-electron interactions play a minimal role for collisions involving low-velocity multicharged-ion impact [7] but can be important at higher impact velocities [8–10]. With regard to the present study, recent experiments in our laboratory using hydrogen, helium, and carbon ions and atoms impacting on helium indicate that two-center electron-electron interactions can be important for very-low-energy (< 10 eV) target electron emission resulting from fast neutral-atom impact but for intermediate-energy electron emission by multiply charged ion impact (the present case), they contribute in a negligible fashion.

Thus, for multicharged-ion impact the problem can be reduced to understanding the passive role which bound projectile electrons play in the collision, i.e., to that of understanding the partial screening of the projectile nuclear charge. Analogous to the situation for fully stripped ion impact, ionization cross sections for partially stripped ion impact are expected to scale with the square of the partially screened projectile charge; but, in the Born description, the degree of screening depends on the momentum transfer. In the semiclassical description, it depends on the impact parameter. This means that we can define a differential *effective* charge, $Z_{\text{eff}}(\varepsilon,\theta)$, as a scaling parameter where ϵ and θ are energy and angle of the emitted electron.

Our measurements of the doubly differential electron emission allows us to study the scaling as a function of electron energy and angle. To obtain information about the scaling as a function of impact parameter, the relationship between the average impact parameter of the collision b_{av} and the emitted electron energy ε can be used [11]. Thus, $b_{\text{av}}=V_p/(\varepsilon+I)$. Here V_p is the projectile velocity and I is the ionization potential of the target electron. Note that this formulation implies that small ejected-electron energies are associated with distant collisions, i.e., large b_{av}, and that large ejected-electron energies imply close collisions, i.e., small b_{av}.

The screening is expected to be rather ineffective for close collisions (where the interaction occurs at distances smaller than the mean orbital radius of the bound electron), but for distant collisions, it should be quite effective [12,13]. This means that electron emission cross sections for very distant collisions should scale as q^2, where q is the net ionic charge of the projectile, and that for very close collisions they should scale as Z^2, independent of the number of electrons bound to the projectile. The reader is again reminded that distant collisions generally result in low-energy electron emission and close collisions typically result in high-energy electron emission.

These expectations are in accordance with data reported some years ago for 2-MeV/u O^{q+}-O_2 collisions [11] and for 0.5-MeV/u He^+ impact [14] on Ar and H_2O. More recently, investigations of 0° electron emission in close collisions involving fully [15] and partially [16] stripped ion impact have verified the expected Z^2 scaling in the binary-encounter region of the emitted electron spectra. However, other recent measurements involving 0° binary-encounter electron emission have demonstrated an "inverse" scaling effect for partially stripped ion impact [17–19]. By inverse scaling, we mean that for fixed Z the binary peak intensity *increases* as *q decreases.* This means that for a particular element, the ionization cross sections for partially ionized projectiles are larger—not smaller—than those for fully stripped projectile impact.

Several theoretical studies of the scaling of cross sections in the binary-encounter region, specifically of the inverse-scaling phenomenon, have been reported in the literature [20–24], and Schultz and Olson [25] have provided predictions for systems yet to be investigated experimentally. Schultz and Olson predict that the degree and type (normal or inverse) of scaling depend on the impact velocity and on the observation angle. For example, ions with impact energies less than a few MeV/u and Z less than approximately 10 are predicted to exhibit inverse scaling at 0°; for higher-Z ions, the effect shifts to higher impact energies. At nonzero laboratory emission angles, they predict that the scaling changes. For example, at 45° the binary-encounter cross sections for 1-MeV/u carbon-ion impact are predicted to be independent of q. Recent measurements by González *et al.* [26], for carbon 4, 5, and 6+ ions impacting on H_2 partially confirm this prediction.

To date, however, all experimental studies demonstrating inverse scaling in the binary-encounter region have used light (H_2 and He) targets and, except for the work just cited, have only studied 0° electron emission. Also they have typically compared cross sections integrated over the binary-encounter peak. The present investigation is more detailed in that we have systematically studied how the differential electron emission cross sections scale as a function of projectile Z, projectile q, laboratory emission angle, ejected-electron energy, and target mass. Specifically, the projectile Z was varied from 5 to 9 while the projectile charge state q ranged from 2 to 5 for B and C impact and from 3 to 6 for O and F impact. Laboratory angles of emission between 10 and 60° were investigated; He, Ne, and Ar targets were studied. In all cases, the impact energy was 0.5 MeV/u and the electron emission was measured from approximately 20 eV to energies well above the binary-encounter peak. The purposes of this study were to investigate how the differential electron emission cross sections scale for distant, as well as for close, collisions and to determine whether previously observed differences between normal and inverse scaling are related to differences in the laboratory emission angles or to the target used.

EXPERIMENTAL PROCEDURE

These experiments were performed at the Pacific Northwest Laboratory using ion beams produced in a small tandem accelerator and then stripped to higher charge states via interactions with a thin carbon foil. Due to hardware and space limitations the stripper foil was located between the accelerator and the analyzing magnet. This placed some restrictions on the maximum charge states of the oxygen and fluorine beams that could be clearly identified and used. Available accelerator energies also restricted the minimum and maximum charge states that we could use for studying 0.5-MeV/u collisions.

The target chamber contained a directed atomic-beam target, a shielded, rotatable, cylindrical-sector electron spectrometer, and a chaneltron detector. Magnetic fields inside the chamber were reduced to less than a few milligauss by double-walled magnetic shielding supplemented with Helmholz coils for further reduction of the vertical field component. Standard techniques were used to collect electron spectra, with and without target gas present. For selected laboratory emission angles data were collected as a function of the emitted electron energy. Electron energies ranged from a few eV to energies well above the binary-encounter peak. However, large background signals, particularly for the smallest emission angles, restricted the usable energy range to 20 eV and above. Lastly, the measured electron spectra were placed on an absolute scale by performing measurements for proton impact and normalizing these data to absolute cross sections previously measured in our laboratory. Primarily due to this normalization process, the cross sections presented here are typically accurate to ±25%.

Since our primary purpose is to investigate how the differential cross sections scale with Z and q, the quantity $Z_{\text{eff}}(\varepsilon,\theta)$ as defined by $Z_{\text{eff}}(\varepsilon,\theta)=[25\,\sigma(\varepsilon,\theta)_{Pq+}/\sigma(\varepsilon,\theta)_{B^{5+}}]^{1/2}$ was determined for each projectile P and charge state q. Here ε is the emitted electron energy and $\sigma(\varepsilon,\theta)_{Pq+}$ are the absolute, doubly differential cross sections that were measured. We recognize that the boron data are influenced to some degree by capture to the continuum for electron velocities near those of the projectile V_p, but since accelerator energy restrictions prohibited us from measuring 0.5-MeV proton impact cross sections, we chose this method to determine $Z_{\text{eff}}(\varepsilon,\theta)$. Since our data, obtained using different projectiles, presumably will be influenced in similar fashion by any unaccounted-for symmetric uncertainties, we feel that investigating $Z_{\text{eff}}(\varepsilon,\theta)$ using only our present measurements provides

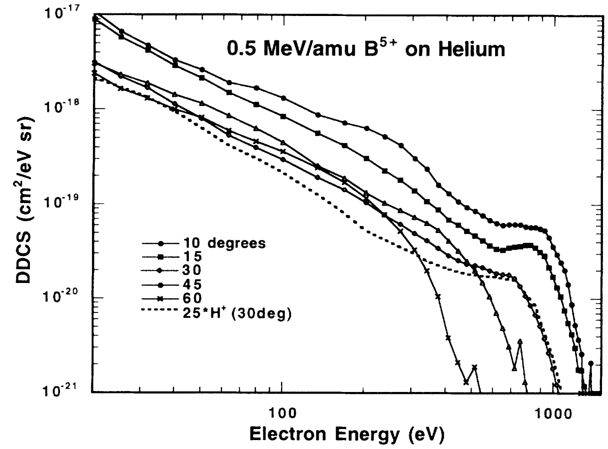

FIG. 1. Absolute doubly differential cross sections for ionizations of helium by 0.5 MeV/u fully stripped boron ions. Also shown for comparison are proton impact cross sections taken from Ref. [27] and scaled by Z^2.

more reliable information about the influence of bound projectile electrons than would comparisons of the present data with other experimental or theoretical work.

RESULTS

A. Fully stripped ion impact

Absolute doubly differential cross sections for selected electron emission angles between 10° and 60° are shown in Fig. 1 for 0.5 MeV/u fully stripped boron ions colliding with helium. Also shown for comparison purposes are 30° cross sections for proton impact [27] which have been scaled by Z^2. These data exhibit features typical for target ionization by fast, fully stripped ion impact, namely an approximately exponential decrease in the cross sections with increasing ejected-electron energy followed by a peak (or shoulder) resulting from binary collisions between the projectile nucleus and a target electron. Above the binary-encounter peak the cross sections rapidly de-

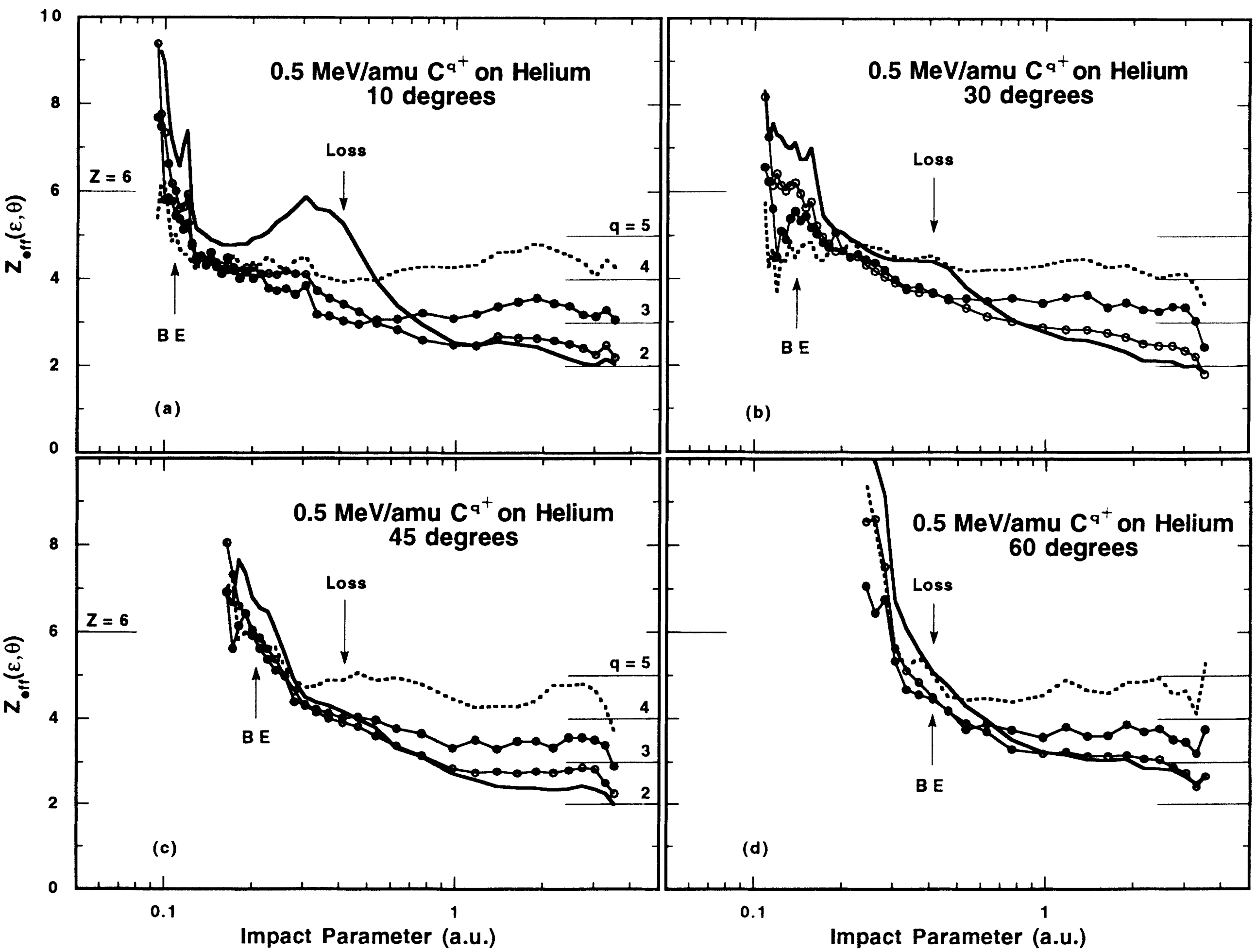

FIG. 2. The effective charge, $Z_{\text{eff}}(\varepsilon,\theta)$, as defined in the text for 0.5-MeV/u C^{q+} ions, $q=2$(——), 3 (○), 4 (●), and 5 (· · ·), interacting with helium. The abscissa is the average impact parameter, which has been determined as described in the text. Arrows indicate the positions of the electron-loss and binary-encounter peaks. The horizontal lines on the left and right sides of the figures indicate the nuclear and net charges of the projectile ions.

crease toward zero.

The binary peak is located approximately at $4T\cos^2\theta$, where T is the reduced projectile energy and θ is the laboratory emission angle. At electron energies where the ejected-electron velocity approximately matches the projectile velocity, roughly 272-eV electron emission in the present case of 0.5 MeV/u, electron capture to the continuum (ECC) processes cause the observed increase in the cross sections. ECC processes are readily evident in the 10° spectrum, but apparently still play an important role at 30° since the boron data are considerably larger than scaled proton impact data in the 100–500-eV region. Lastly, Doppler-shifted projectile Auger emission is responsible for the peaks in the cross sections near 500 and 750 eV for 60° and 45° emission, respectively, and for the shoulder near 1200 eV in the 10° data.

B. Partially stripped ion impact on helium

In Fig. 2, data for C^{q+} impact on helium are shown. For ease in comparison at different angles of emission and in order to investigate scaling properties, $Z_{\rm eff}(\varepsilon,\theta)$ is plotted versus $b_{\rm av}$, where $Z_{\rm eff}(\varepsilon,\theta)$ and $b_{\rm av}$ are determined as described above. Uncertainties in the $Z_{\rm eff}(\varepsilon,\theta)$ values primarily result from statistical uncertainties in the cross sections used in their determination since experimental conditions—e.g., target-gas pressure, electron detection efficiency, and solid angle—are the same for both the partially stripped and fully stripped ion impact data. Generally this leads to uncertainties in $Z_{\rm eff}(\varepsilon,\theta)$ of less than 10% except for the highest-energy electrons (smallest impact parameters) investigated where the cross sections become immeasurably small and for electron energies below 20 eV ($b_{\rm av} > 3$ a.u.), where background signals sometimes are large. Expected centroid positions for binary-encounter and electron-loss or ECC processes are indicated by the arrows. The horizontal lines and values near the left and right axes respectively indicate q and Z values for the various projectiles used.

Let us first concentrate on distant collisions which predominantly lead to the emission of low-energy electrons. Here we expect the projectile electron screening to reduce the cross sections with respect to those resulting from bare ion impact. These and similar data for oxygen-ion impact [28] demonstrate this feature. They also show that for collisions occurring at mean distances larger than carbon K and L shells, roughly 0.2 and 0.7 a.u. respectively, $Z_{\rm eff}(\varepsilon,\theta)$ attains a nearly constant value. This occurs for all angles of emission. For distant collisions, the data indicate that $Z_{\rm eff}(\varepsilon,\theta) > q$ for low-charge-state ions but $Z_{\rm eff}(\varepsilon,\theta) < q$ for more highly stripped ions. We note that these observations may in part be influenced by the fact that we used cross sections for B^{5+}, rather than for proton impact, to determine $Z_{\rm eff}(\varepsilon,\theta)$. For example, in Fig. 1 the 30° boron data are approximately 20% larger than the scaled proton data. Thus, had we used the proton data in determining $Z_{\rm eff}(\varepsilon,\theta)$, the values would be approximately 10% larger than shown. This would mean that, for distant collisions, $Z_{\rm eff}(\varepsilon,\theta) \approx q$ for large q and $Z_{\rm eff}(\varepsilon,\theta) > q$ for small q, which is more in line with expectations from a simple physical screening picture.

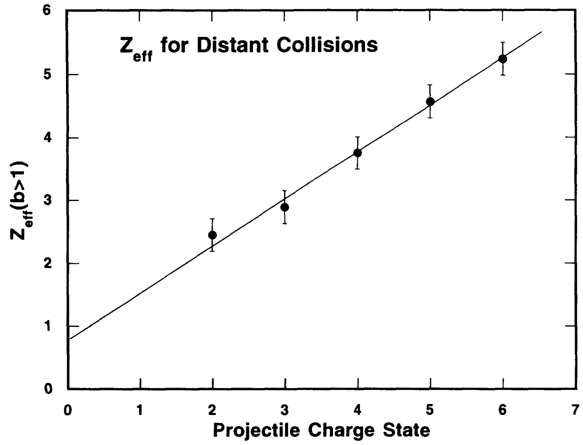

FIG. 3. The average effective charge for partially stripped projectiles inducing ionization via distant collisions. The data are average values obtained from 0.5-MeV/u multiply charged ions of boron, carbon, oxygen, and fluorine colliding with helium. The data are also averaged over angles of emission between 10° and 60° and impact parameters between 1.5 and 3 a.u. The line serves to guide the eye. Note that a systematic 10% increase in $Z_{\rm eff}(b>1)$ may be necessary since the partially stripped ion impact data were referenced to B^{5+}, rather than proton, cross sections.

As the average impact parameter decreases, the electron clouds of the colliding particles begin to overlap. This decreases the screening and $Z_{\rm eff}(\varepsilon,\theta)$ increases. From a simple geometric picture, carbon K- and L-shell screening effects should diminish for impact parameters smaller than 0.2 and 0.7 a.u. respectively. This leads to the observed increases in $Z_{\rm eff}(\varepsilon,\theta)$ for C^{2+},C^{3+} and for C^{4+},C^{5+} projectiles in these regions. For low-charge-state ions possessing weakly bound electrons, projectile ionization also contributes to the forward emission cross

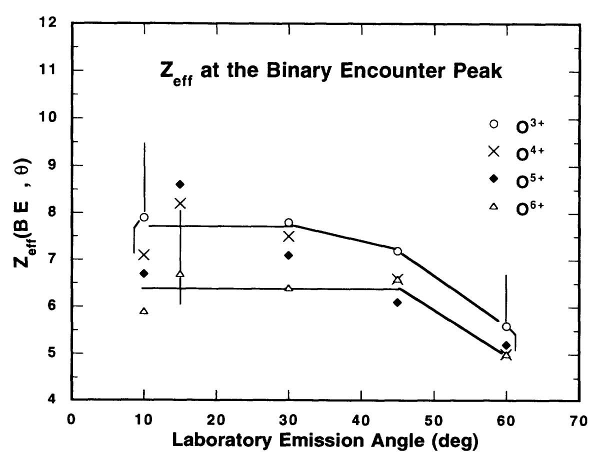

FIG. 4. $Z_{\rm eff}(\varepsilon,\theta)$ at the binary-encounter peak position for 0.5-MeV/u oxygen ions colliding with helium. The lines through the O^{3+} and O^{6+} data serve simply to guide the eye. Representative experimental uncertainties for the 3+ and 6+ data are shown.

section which influences $Z_{\rm eff}(\varepsilon,\theta)$ as indicated by the structures designated by the arrow labeled "Loss."

For electron emission in the binary-encounter region indicated by the arrow labeled "BE", $Z_{\rm eff}(\varepsilon,\theta)$ increases sharply. Previous experimental studies have only investigated how the integral binary-encounter peak intensity or the centroid intensity scale. The present data demonstrate that $Z_{\rm eff}(\varepsilon,\theta)$ is considerably larger on the high-energy (small b) side of the peak than on the low-energy (larger b) side. These data also show that $Z_{\rm eff}(\varepsilon,\theta)$ exceeds Z for very close collisions. This should be investigated further using data accumulated with higher statistics. The reader should note that relating the momentum transfer to an average impact parameter may be questionable for very close binary collisions, which means the "small impact parameter" information should be regarded in a qualitative rather than a quantitative manner.

At the binary peak position, $Z_{\rm eff}(\varepsilon,\theta)$ decreases with q at small θ but tends to be nearly independent of q for larger θ. This is in accordance with the predictions of Schultz and Olson [25] and recent observations by González *et al.* [26]. However, for 60° emission, $Z_{\rm eff}(\varepsilon,\theta)$ increases with q for $q\geq 4$, whereas for lower charge states $Z_{\rm eff}(\varepsilon,\theta)$ decreases with q, assuming of course that $Z_{\rm eff}(\varepsilon,\theta)=6$ for fully stripped carbon impact. Inverse scaling (where the cross sections decrease for increasing q) is found at 45° only for $q<3$.

Figure 3 investigates $Z_{\rm eff}(\varepsilon,\theta)$ for distant collisions in more detail. For distant collisions, Fig. 2 demonstrates that $Z_{\rm eff}(\varepsilon,\theta)$ was nearly constant for all angles of emission when the impact parameter was larger than 1 a.u. Thus average values of $Z_{\rm eff}(\varepsilon,\theta)$ were determined for each projectile, projectile charge state, and angle of emission using data for impact parameters ranging from 1.5 to 3 a.u. Within experimental uncertainties, these average values depended only on the projectile charge q and not on the projectile type or angle of emission. Hence, the effective charges for distant collisions designated by $Z_{\rm eff}(b>1)$ that are displayed in Fig. 3 are average values for all angles and projectiles investigated.

As discussed above, these data indicate that for distant collisions, low-charge-state partially stripped projectiles interact with an effective charge that is larger than the net ionic charge q, but highly stripped projectiles interact with an effective charge that is smaller than q. However, we again emphasize that B^{5+}, rather than proton, impact data were used in determining $Z_{\rm eff}(\varepsilon,\theta)$. This may result in systematic underestimations of $Z_{\rm eff}(\varepsilon,\theta)$ and, hence, of $Z_{\rm eff}(b>1)$ by approximately 10%, which would mean that in distant collisions highly stripped projectiles interact with an effective charge that is nearly the same as the net ionic charge.

In Fig. 4 the angular dependence of the effective charge for close collisions—specifically at the binary-encounter peak, $Z_{\rm eff}({\rm BE},\,\theta)$—is investigated using the oxygen impact data. The solid lines serve only to guide the eye through the O^{3+} and O^{6+} data. Representative experimental uncertainties are indicated. These result from relative uncertainties in the cross sections for different charge states at a particular angle that lead to relative uncertainties of approximately ±10% in $Z_{\rm eff}({\rm BE},\,\theta)$ and systematic uncertainties, as discussed above, of +10%. Although the experimental uncertainties overlap, the general trends exhibited by these data are an inverse scaling at small angles of emission changing to normal scaling for more highly stripped ion impact and larger angles of emission. As a function of angle, $Z_{\rm eff}({\rm BE},\,\theta)$ is rather constant for smaller angles of emission but decreases in value for larger angles of emission.

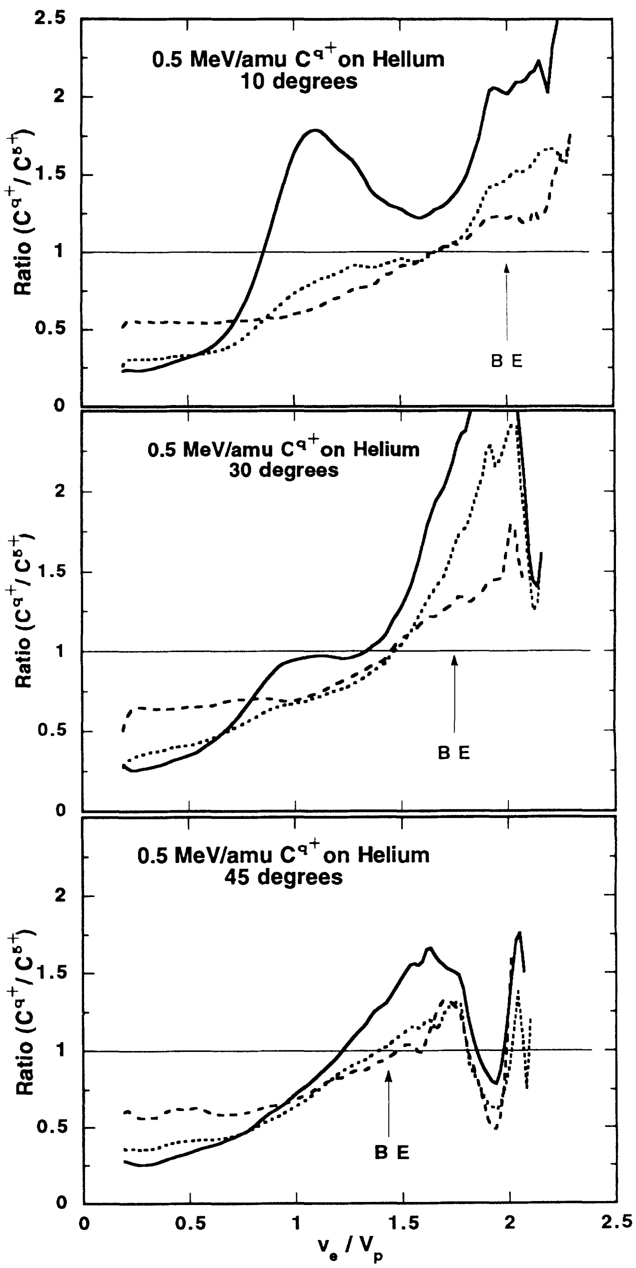

FIG. 5. Doubly differential cross section ratios for 0.5-MeV/u carbon ions colliding with helium as a function of v_e/V_p and emission angle. The ratios C^{q+}/C^{5+} are for $q=2$, ——; 3, · · · ; and 4, — — —, respectively. Expected locations of the binary-encounter peak are indicated by arrows.

C. Partially stripped carbon-ion impact on other targets

In order to provide additional systematics about scaling of differential electron emission cross sections resulting from multicharged ion impact on heavier targets, cross sections were measured for C^{q+} ($q=2$ to 5) impact on Ne and Ar. For the heavier targets, fully stripped ion impact data were not measured. Thus, simple ratios of cross sections referenced to the C^{5+} data were determined rather than values for $Z_{\text{eff}}(\varepsilon,\theta)$, as was done for the helium target. Nevertheless, these data can still be used to provide information about how projectile electrons influence target ionization as the asymmetry of the collision system changes. These ratios, as a function of the ejected-electron velocity divided by the projectile velocity v_e/V_p, are shown for several emission angles in Figs. 5–7 for He, Ne, and Ar targets, respectively. Note that at 10° and 30°, the ratios for small q are strongly influenced by electron capture and loss processes in the region near $v_e/V_p=1$.

For electrons emitted with velocities less than V_p, which corresponds to distant collisions, the cross-section ratios depend only on q, independent of emission angle or target. For close collisions, corresponding to $v_e > V_p$, target and angular dependent differences are seen. Ionization of helium, for example, exhibits large inverse-scaling effects at small angles of emission, but these effect are less dramatic at larger angles. For argon, inverse-scaling effects are smaller, and these effects also decrease at larger emission angles. Neon, on the other hand, demonstrates inverse-scaling effects more clearly for larger an-

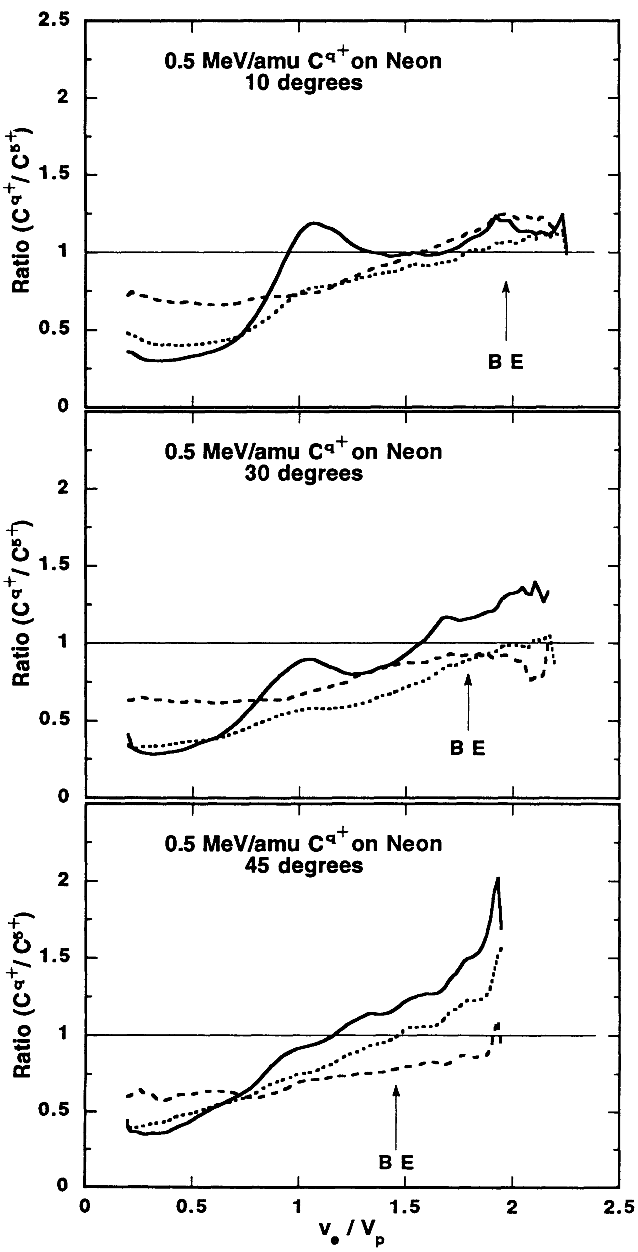

FIG. 6. Same as Fig. 5 but for a neon target.

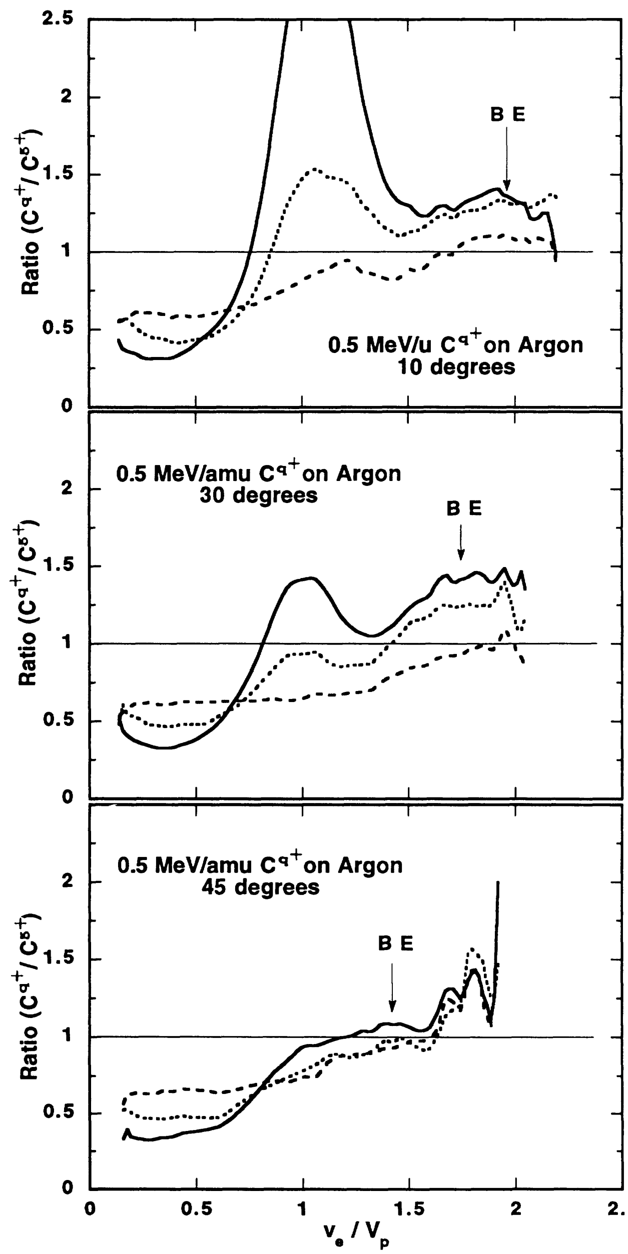

FIG. 7. Same as Fig. 5 but for an argon target.

gles of emission. Therefore, these limited data demonstrate no obvious systematic trends in how cross sections scale for close collisions.

CONCLUSIONS

This study of differential electron emission in multicharged, partially stripped, ion-atom collisions has shown that for distant collisions, i.e., for low-energy secondary-electron production, the cross sections scale as $(q')^2$, where $q' > q$ when q is small; for more highly stripped ion impact the cross sections scale as $(q')^2$, where $q' < q$. These observations, which were obtained by referencing the partially stripped ion impact data to fully stripped boron ion, rather than proton, impact data, may be subject to a systematic underestimation of approximately 10%, which would imply that the cross sections for highly stripped ion impact may scale approximately as q^2 while the cross sections for low-charge-state ion impact scale as $(q')^2$ where $q' > q$. For energetic electron emission in the forward direction, specifically for electrons emitted from helium as the result of binary collisions between a target electron and the projectile nucleus, the cross sections were found to systematically increase as electrons were added to a bare projectile ion. At larger laboratory emission angles this inverse-scaling effect disappeared, at least for higher charge states of the ions investigated in this study. For still closer collisions, the differential cross sections always increased as electrons were added to the projectile ion. This occurred for all targets and emission angles investigated, but the increase was more dramatic for the lightest target studied.

ACKNOWLEDGMENTS

This work was supported in part by the Office of Health and Environmental Research, U.S. DOE, Contract No. DE-AC06-76RLO-1830, the Willkomm-Stiftung, and BMFT.

[1] L. H. Toburen, *Physical and Chemical Mechanisms in Molecular Radiation Biology*, edited by W. A. Glass and M. N. Varma (Plenum, New York, 1991), pp. 51–97.

[2] N. Stolterfoht, D. Schneider, J. Tanis, H. Altevogt, A. Salin, P. D. Fainstein, R. Rivarola, J. P. Grandin, J. H. Scheurer, S. Andriamonje, D. Bertault, and J. F. Chemin, Europhys. Lett. **4**, 899 (1987).

[3] D. Schneider, D. DeWitt, A. S. Schlachter, R. E. Olson, W. G. Graham, J. R. Mowat, R. D. DuBois, D. H. Loyd, V. Montemayor, and G. Schiwietz, Phys. Rev. A **40**, 2971 (1989).

[4] D. H. Schneider, D. R. DeWitt, R. W. Bauer, J. R. Mowat, W. G. Graham, A. S. Schlachter, B. Skogvall, P. Fainstein, and R. D. Rivarola, Phys. Rev. A **46**, 1296 (1992).

[5] H. K. Haugen, L. H. Andersen, P. Hvelplund, and H. Knudsen, Phys. Rev. A **26**, 1950 (1982).

[6] J. O. Pedersen, P. Hvelplund, A. G. Petersen, and P. D. Fainstein, J. Phys. B **24**, 4001 (1991).

[7] S. T. Manson and R. D. DuBois, Phys. Rev. A **46**, R6773 (1992).

[8] W. E. Meyerhof, H. P. Hülskötter, Q. Dai, J. H. McGuire, and Y. D. Wang, Phys. Rev. A **43**, 5907 (1991).

[9] T. J. M. Zouros, D. H. Lee, and P. Richard, Phys. Rev. Lett. **62**, 2261 (1989).

[10] C. P. Bhalla and R. Shingal, J. Phys. B **24**, 3187 (1991).

[11] N. Stolterfoht, *Structure and Collisions of Ions and Atoms*, edited by I. A. Sellin (Springer-Verlag, Berlin, 1978), p. 155.

[12] J. H. McGuire, N. Stolterfoht, and P. R. Simony, Phys. Rev. A **24**, 97 (1981).

[13] L. H. Toburen, N. Stolterfoht, P. Ziem, and D. Schneider, Phys. Rev. A **24**, 1741 (1981).

[14] L. H. Toburen and W. E. Wilson, Phys. Rev. A **19**, 2214 (1979); Radiat. Res. **82**, 27 (1980).

[15] D. H. Lee, P. Richard, T. J. M. Zouros, J. M. Sanders, J. L. Shinpaugh, and H. Hidmi, Phys. Rev. A **41**, 4816 (1990).

[16] Y. Kanai, T. Kambara, M. Oura, Y. Zou, S. Kravis, and Y. Awaya, in *Abstracts of VI International Conference on the Physics of Highly Charged Ions*, Manhattan, KS, 1992, edited by P. Richard, M. Stöckli, C. L. Cocke, and C. D. Lin (AIP, New York, 1992), pp. 315–318.

[17] P. Richard, D. H. Lee, T. J. M. Zouros, J. M. Sanders, and J. L. Shinpaugh, J. Phys. B **23**, L213 (1990).

[18] O. Jagutzki, S. Hagmann, H. Schmidt-Böcking, R. E. Olson, D. R. Schultz, R. Dörner, R. Koch, A. Skutlartz, A. González, T. B. Quinteros, C. Kelbch, and P. Richard, J. Phys. B **24**, 2579 (1991).

[19] T. B. Quinteros, A. D. González, O. Jagutzki, A. Skutlartz, D. H. Lee, S. Hagmann, P. Richard, C. Kelbch, S. I. Varghese, and H. Schmidt-Böcking, J. Phys. B **24**, 1377 (1991).

[20] C. O. Reinhold, D. R. Schultz, and R. E. Olson, J. Phys. B **23**, L591 (1990).

[21] K. Taulbjerg, J. Phys. B, **23**, L761 (1990).

[22] C. O. Reinhold, D. R. Schultz, R. E. Olson, D. Kelbch, R. Koch, and H. Schmidt-Böcking, Phys. Rev. Lett. **66**, 1842 (1991).

[23] R. Shingal, Z. Chen, K. R. Karim, C. D. Lin, and C. P. Balla, J. Phys. B **23**, L637 (1990).

[24] H. I. Hidmi, C. P. Bhalla, S. R. Grabbe, J. M. Sanders, P. Richard, and R. Shingal, Phys. Rev. A **47**, 2398 (1993).

[25] D. R. Schultz and R. E. Olson, J. Phys. B **24**, 3409 (1991).

[26] A. D. González, P. Dahl, P. Hvelplund, and K. Taulbjerg, J. Phys. B **25**, L573 (1992).

[27] M. E. Rudd, L. H. Toburen, and N. Stolterfoht, At. Data Tables **18**, 413 (1976).

[28] R. D. DuBois, L. H. Toburen, M. E. Middendrof, and O. Jagutzki, in *AIP Proceedings of VIth International Conference on the Physics of Highly-Charged Ions, Manhattan, KS, 1992*, edited by P. Richard, M. Stöckli, C. L. Cocke, and C. D. Lin, AIP Conf. Proc. No. 274 (AIP, New York, 1992), pp. 327–30.